

Article

Aluminum Removal from Rare Earth Chloride Solution through Regulated Hydrolysis via Electrochemical Method

Yaoyao Zhu^{1,2}, Jian Li^{2,3}, Dongyue Xie^{1,2}, Hui Zhang^{1,2,3,*}, Man Li^{1,2}, Binfeng Xu^{1,2}, Xuxia Zhang^{2,3}, Yangyang Xie^{2,3} and Tao Qi^{1,2,3,*}

¹ School of Rare Earths, University of Science and Technology of China, Hefei 230026, China; yyzhu21@gia.cas.cn (Y.Z.); dyxie21@gia.cas.cn (D.X.); mli22@gia.cas.cn (M.L.); bfxu22@gia.cas.cn (B.X.)

² Ganjiang Innovation Academy, Chinese Academy of Sciences, Ganzhou 341000, China; jli@gia.cas.cn (J.L.); xxzhang@gia.cas.cn (X.Z.); yyxie@gia.cas.cn (Y.X.)

³ Jiangxi Province Key Laboratory of Cleaner Production of Rare Earths, Ganzhou 341000, China

* Correspondence: zhanghv@ipe.ac.cn (H.Z.); tqigreen@ipe.ac.cn (T.Q.)

Abstract: Due to the coexistence of Al³⁺ and RE³⁺ and their similar properties, the separation of aluminum from rare earths is difficult. In this study, selective precipitation was used to separate aluminum from rare earth chloride solution via electrochemical regulated hydrolysis. By controlling the current density and electrolytic time, the rate of hydroxyl ion production was regulated, and the selective separation of rare earth and aluminum was realized according to the different precipitation sequences. By altering the temperature, current density, pH value, and other parameters, the separation performance of aluminum from rare earth in mixed rare earth chloride systems was systematically investigated. The removal rate of aluminum reached 88.35%, and the loss rate of rare earth was only 5.99% under optimized conditions. Compared with traditional neutralization hydrolysis, the new process showed higher efficiency and lower rare earth loss rate. Furthermore, a kinetic analysis of aluminum precipitation revealed that the reaction adhered to pseudo-first order kinetics. Additionally, the precipitate obtained via separation and filtration was amorphous alumina hydroxide with a small amount of rare earth attached. No reagent was consumed for the new process, which was more efficient and cleaner, providing a new idea for removing aluminum impurities from rare earth solutions.

Keywords: aluminum; rare earth; separation; regulated hydrolysis; electrochemical



Citation: Zhu, Y.; Li, J.; Xie, D.; Zhang, H.; Li, M.; Xu, B.; Zhang, X.; Xie, Y.; Qi, T. Aluminum Removal from Rare Earth Chloride Solution through Regulated Hydrolysis via Electrochemical Method. *Separations* **2024**, *11*, 149. <https://doi.org/10.3390/separations11050149>

Academic Editor: Anastasios Zouboulis

Received: 16 April 2024

Revised: 3 May 2024

Accepted: 10 May 2024

Published: 12 May 2024



Copyright: © 2024 by the authors. Licensee MDPI, Basel, Switzerland. This article is an open access article distributed under the terms and conditions of the Creative Commons Attribution (CC BY) license (<https://creativecommons.org/licenses/by/4.0/>).

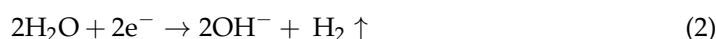
1. Introduction

Driven by rapidly increasing industrial activities, the materials of rare earths (REs) have become the focus of attention [1–3]. REs are attractive due to their great promise with regards to unique magnetic, electronic, and optical properties arising from their 4f valence electron shell [4–6]. Due to the low content of REs in the leaching solution, the chemical precipitate method is adopted in the industry for the purification and obtaining of RE compounds containing 92% REO and 1.5% Al impurity [7]. The RE compounds are leached via HCl solution for the raw material preparation for the solvent extraction process [8]. However, the Al impurities in the HCl leachate must be removed further, because the significant accumulation of Al in extractant systems causes the emulsification of extractant and reduced extraction of RE [7,9,10].

The separation of RE and Al is challenging due to their similar chemical properties [11]. Solvent extraction and selective precipitation are commonly used in industry to separate Al and RE. Solvent extraction has been proved to be an efficient way to separate Al and different conventional extraction systems (naphthenic acid, P204, P507) have been investigated thoroughly to promote Al removal in RE leachate [12–14]. In recent years, a novel functionalized ionic liquid ([DOC4 mim][DEHG]) has been employed for the separation of aluminum from rare earth leaching solutions; the removal rate of aluminum achieved 95%

and the recovery rate of rare earth reached 96% [15]. However, the stability of some new extractants and water contamination caused by the dissolution of the extractant are still issues that need to be further considered [16]. Selective precipitation is a conventional choice for selective removal of Al by the addition of alkali compounds (ammonium bicarbonate [17], sodium hydroxide [18], and alkaline calcium/magnesium compounds [19,20]). Al removal efficiency can reach 97% by regulating a suitable pH in the solution [21]. Research has demonstrated that certain organic compounds, which contain carboxyl, hydroxyl, amino, and other functional groups, can form stable complexes with Al^{3+} , Fe^{3+} , Cu^{2+} , Ca^{2+} , Ni^{2+} , Cr^{3+} , and other metal ions in aqueous solutions under certain conditions [22–24]. The results revealed that Al^{3+} removal reached 94.39%, and RE^{3+} loss was only 8.21% [22]. However, the loss of RE is unavoidable due to the similar precipitate properties in both Al^{3+} and RE^{3+} and the excessive precipitate reagents may dissolve in the acidic leaching solution which is not favorable for subsequent extraction processes.

In recent years, electrochemical precipitation has been the focus of much research attention on the separation of the impurities in solutions due to its environmental compatibility and versatility [25]. The procedure necessitates the production of a high concentration of hydroxide ions in the vicinity of the cathode through water electrolysis, which can be articulated as follows:



The hydroxide ions are believed to play crucial roles in harnessing ion removal via the following reactions:



where M is metallic ions including Ca^{2+} , Mg^{2+} , Fe^{3+} , Al^{3+} , and so on [26]. The electrochemical removal of Al from rare earth sulfate leachate with low concentration of RE has been developed recently [27]. However, the removal of Al from the rare earth chloride solutions has not been investigated.

In this study, the speed of producing hydroxyl ions was controlled by regulating the current density, which regulates pH to achieve the selective separation. A new double-membrane three-compartment electrolytic reactor was designed for preventing the diffusion of Cl^- in the HCl leachate and avoided the production of Cl_2 on the anodes. By studying the effect of various parameters (such as pH of the solution, current density, and temperature) on the regulated hydrolysis with an electrochemical method, the optimal experimental conditions were determined. The precipitation kinetics of aluminum and the morphological characterisation of the resulting precipitate were discussed, and the energy consumption and green chemical evaluation of the experiment were determined.

2. Materials and Methods

2.1. Materials and Reagents

The rare earth chloride solution (RECl_3) was kindly supplied by China Rare Earth Group Co., Ltd. (Jiangxi, China); the composition is shown in Table 1. The concentration of H^+ was more than 1 mol/L. Sulfuric acid and ammonia chloride were purchased from Shanghai Sinopharm reagent. The titanium sheet and titanium platinum-plated electrodes were selected as the cathode and anode plates, respectively.

Table 1. The composition of the rare earth chloride solution (g/L).

Elements	Concentrations
La	22.76
Ce	3.07
Pr	6.69
Nd	24.13
Sm	6.15
Eu	0.67
Gd	6.08
Tb	1.21
Dy	6.79
Ho	1.36
Er	4.10
Tm	0.63
Yb	4.24
Lu	0.52
Y	32.70
Al	4.38

2.2. Instrumentation

Inductively coupled plasma emission spectrometry (ICP-OES, PQ9000, Analytikjena, Jena, Germany) was used to detect the concentrations of Al^{3+} and RE^{3+} in the aqueous phase after the regulated hydrolysis experiments. All the pH values mentioned in this paper were obtained via the digital pH meter pHS-3E (Shanghai INESA Analytical Instrument CO., Ltd., Shanghai, China). The morphology of the precipitation was characterized via scanning electron microscope and transmission electron microscope (JSM-IT800). The process of removing aluminum impurities from rare earth solutions was performed in a magnetic stirrer (ZNCL-2DB*6, Qiuzuo Instrument Equipment Co., Ltd., Henan, China) at a speed of 300 r/min. The distribution and morphology of Al(III) in solution were simulated via Visual MINTEQ 3.1 (Jon Petter Gustafsson) software.

2.3. Procedure

The electrolytic cell was divided with three distinct compartments, separated by anionic and cationic membranes. These compartments were designated as the anode chamber, middle chamber, and cathode chamber, respectively.

A certain concentration of sulfuric acid solution was introduced into the anode chamber. Concurrently, an ammonium chloride solution with a particular concentration was added to the middle chamber. For the cathode chamber, a rare earth chloride solution containing aluminum impurities was utilized. Prior to its introduction, to improve electrolytic efficiency, rare earth ore concentrates ($\text{RE}_2(\text{CO}_3)_3$) were added to adjust the pH prior to electrochemically selective precipitation for aluminum removal. A total of 100 mL of the mixed rare earth chloride solution was poured into a beaker, a certain amount of rare earth ore concentrate (about 2.5 g) was added; this was stirred evenly for 10 min; the pH was adjusted to 2.70; it was then filtered and the cathodic solution was obtained for electrolysis. The concentration changes of each element after pH adjustment are shown in Table 2. When the rare earth oxides were added, the concentration of rare earth in the solution increased to 197.91 g/L, and the concentration of aluminum ion increased correspondingly to 5.42 g/L.

Table 2. The composition of the rare earth chloride solution after pH adjustment (g/L).

Elements	Concentrations
La	46.16
Ce	4.06
Pr	11.80
Nd	44.34
Sm	9.67
Eu	1.32
Gd	8.92
Tb	1.71
Dy	9.15
Ho	1.79
Er	4.99
Tm	0.76
Yb	5.02
Lu	0.55
Y	47.74
Al	5.42

The whole technical route is shown in Figure 1. Electrolysis was executed using direct current, and in order to prevent local alkalosis, mechanical stirring was performed on its catholyte throughout the electrolysis process, and sampling, measuring pH, and filtering tests were carried out on the obtained samples at intervals. Figure 2 shows a diagram of the cell and the electrolysis process. The anode was connected with the positive electrode of the power supply, and an oxygen evolution reaction occurred on the surface of the electrode, which is shown in Reaction (1). Correspondingly, the hydrogen evolution reaction occurred at the surface of the cathode electrode connected to the negative electrode of the power supply, and the reaction is expressed as follows.

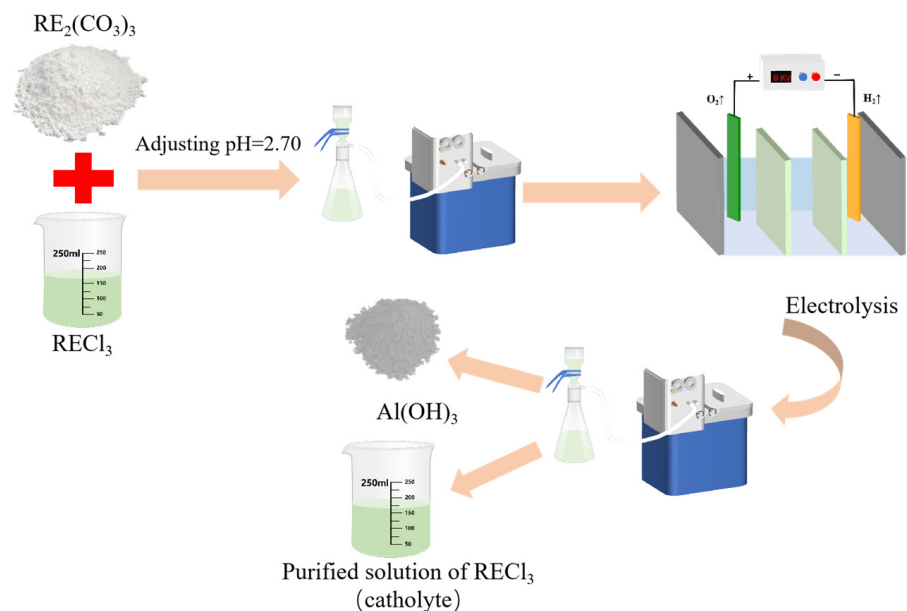


Figure 1. Flow chart of removal of aluminum from rare earth chloride solution.

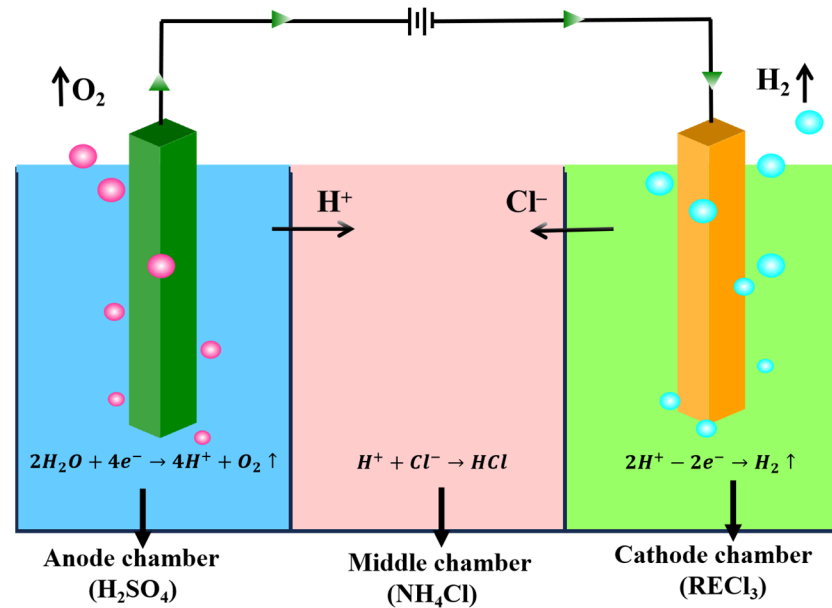


Figure 2. The diagram of electrolysis cell and electrolysis process.

The removal ratios of the impurities (R) and the loss ratio of RE³⁺ (L) were calculated using the following equations:

$$R = \left(1 - \frac{C_{eq,im}}{C_{init,im}}\right) \times 100\% \tag{5}$$

$$L = \left(1 - \frac{C_{eq,RE}}{C_{init,RE}}\right) \times 100\% \tag{6}$$

where $C_{init,im}$ and $C_{eq,im}$ are the concentrations of impurities in initial and final aqueous, respectively. $C_{init,RE}$ and $C_{eq,RE}$ are the concentrations of RE³⁺ in initial and final aqueous, respectively.

3. Results and Discussion

3.1. Optimization

3.1.1. Effect of Temperature

It is known that temperature conditions exert major influences on chemical reactions. Therefore, the influence of reaction temperature on the removal efficiency of aluminum from rare earth solutions was investigated. Figure 3 illustrates the correlation between reaction temperature, aluminum-removal rate, and rare earth loss rate. As can be seen from this figure, increasing the temperature was not conducive to removing aluminum; meanwhile, the higher the temperature, the greater the loss of rare earth due to the high concentration of rare earth. The effect of changing temperature on hydrolysis of rare earths cannot be ignored. For example, in the early 1980s, Miller extensively studied the factors affecting the adsorption of lanthanides by montmorillonite and found that the degree of irreversible adsorption increased with higher temperatures, which was attributed to temperature-induced hydrolysis of the rare earth elements, as higher temperatures would force the hydrated lanthanides adsorbed on the clay surface to partially dehydrate [28]. This process was called “temperature-enhanced cationic hydrolytic fixation”, and the increase in temperature caused the hydrolysis pH of the rare earth elements to move to a lower value [29]; this also confirmed that the rise in temperature accelerated the hydrolysis of rare earths, resulting in a large loss of rare earths. This shows that the electrochemical selective hydrolysis method at room temperature can reduce the loss of REs and enhance the removal of Al impurities, which was advantageous for both environmental protection and cost reduction.

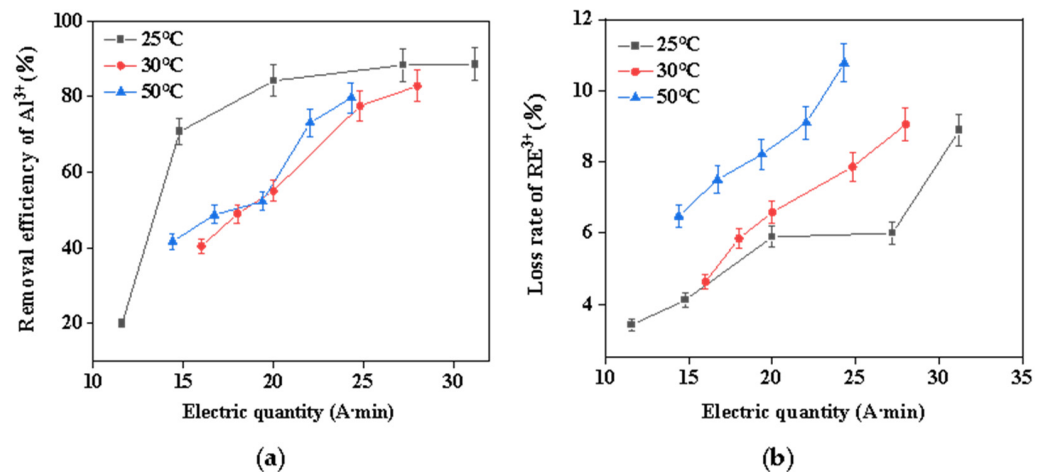


Figure 3. (a) Effect of temperature on the removal efficiency of Al³⁺; (b) effect of temperature on the loss rate of RE³⁺.

3.1.2. Effect of Current Density

During the electrochemical precipitation process, the concentration of hydroxide ions significantly influences both the rate of hydrolysis and the efficiency of mass transfer between electrolytes and electrodes. The production rate of hydroxyl ions was contingent upon the regulation of varying current densities [30]. Consequently, this study examined the impact of different current densities on the removal of aluminum impurities from rare earth chloride solution. Figure 4 shows the relationship between the rare earth loss rate, the aluminum-removal rate, and electric quantity at different current densities. Throughout the electrochemical selective precipitation process, the precipitation rate increased rapidly and then gradually slowed down as the electric quantity inputted increased. When the electric quantity was less than 20 A·min, the reaction produced hydroxide precipitation rapidly. According to the proposed electrochemical mechanism, with the increase in current density and electrolysis time, more OH⁻ was produced nearby the cathode, and the electromigration of ions was enhanced, resulting in more ions forming precipitation near the cathode surface. The precipitation rate then increased relatively slowly, mainly because the precipitation was limited by the mass transfer of Al³⁺, RE³⁺, and OH⁻ [31]. As the amount of electricity and current density increased, so did the rare earth loss rate. This was mainly because excessive current density led to an increase in the OH⁻ production rate, which further rapidly increased the pH near the cathode plate, inevitably resulting in a large loss of rare earth. At the same time, it can be seen in Figure 4a that the rapid hydrolysis of RE³⁺ seemed to have a negative effect on the removal of aluminum. It was speculated that the reason for this was that the hydroxyl ions produced on the electrode surface react preferentially with rare earth ions, thus inhibiting their diffusion into the bulk solution and reducing the consumption of hydroxyl by Al³⁺ [27]. Although the low current density was found to be beneficial for the removal of aluminum impurities and rare earths, the optimum current density was determined to be 100 A/m², taking into account the reaction efficiency.

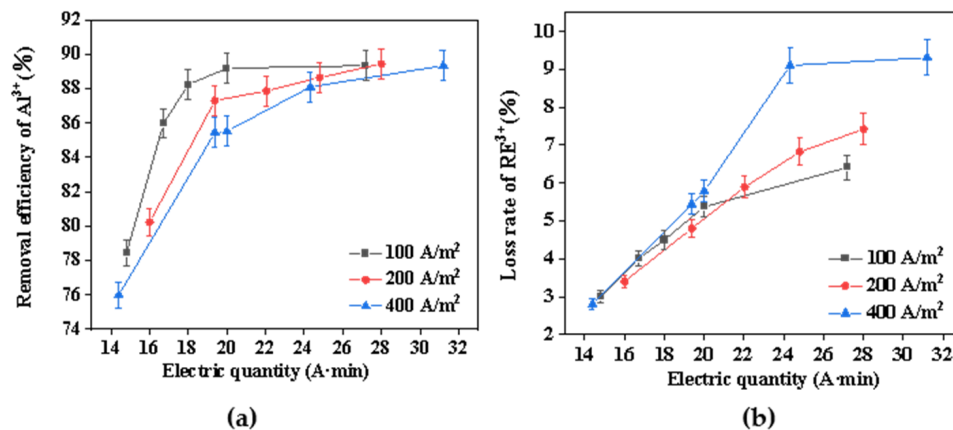


Figure 4. (a) Effect of current density on the removal efficiency of Al^{3+} ; (b) effect of current density on the loss rate of RE^{3+} .

3.1.3. Effect of Final pH

During the electrochemical precipitation process, the equilibrium pH has a great influence on the impurity-removal efficiency. The pH of the rare earth chloride solution, which contained aluminum impurities, was initially 2.70 prior to electrolysis. After electrolysis, hydroxide ions were generated continuously and in a controlled manner, thereby elevating the pH of the solution. It had been proposed that hydrated metal ions are essentially acids by Lewis acids and bases. Consequently, the formation process of metal ion hydroxide precipitation can be regarded as a process of step reaction between the metal ion and the hydroxide ion [32,33]. The existing forms of Al^{3+} in aqueous solution exhibit various states, the partial equilibrium reaction can be expressed via Equations (7)–(9) [16]. As can be seen from the equations given, an increase in the pH of the solution results in a decrease in the concentration of H^+ . Consequently, the equilibrium is shifted to the right. Under these conditions, the formation of $Al(OH)_3$ is more likely.



In order to explore the optimal pH for the separation of Al^{3+} and RE^{3+} , its effect on removing aluminum and the loss rate of rare earth were also investigated. At the same time, the distribution and the shape of the Al(III) were simulated via the Visual MINTEQ 3.1 software. The result is shown in Figure 5. From Figure 5a, within the pH ranging from 3.20 to 4.01, the rate of aluminum removal exhibited a significantly steeper slope compared with that of rare earth loss. When the pH value reached 3.90, the removal rate of aluminum was 88.3%, while the loss rate of rare earth was only 5.99%. It can be concluded that because the electrolyte will produce a large amount of OH^- during the electrolysis process, the pH value will increase, resulting in the hydrolysis of metal ions producing a large amount of precipitation. However, when the pH value continued to rise, the removal rate of aluminum was basically unchanged, and the loss rate of rare earth increased significantly. Meanwhile, as shown in Figure 5b, Al(III) in solution existed mainly in the form of Al^{3+} , $Al(OH)_2^+$, $Al(OH)_4^-$, and $AlOH^{2+}$. The content of Al^{3+} in the solution was highest and its ability to bind OH^- was strongest when the pH of the solution was less than 3. With increasing pH, $AlOH^{2+}$ gradually increased, resulting in a weakening of the ability of complex OH^- . As the pH rose to around 4, $Al(OH)_2^+$ began to appear in the solution, further reducing the ability to bind OH^- . The excess OH^- combined with the rare earth caused a large loss of rare earth ions. Therefore, by controlling the electrochemical precipitation process, the final pH was adjusted to 3.90, which was conducive to the separation of aluminum and rare earths.

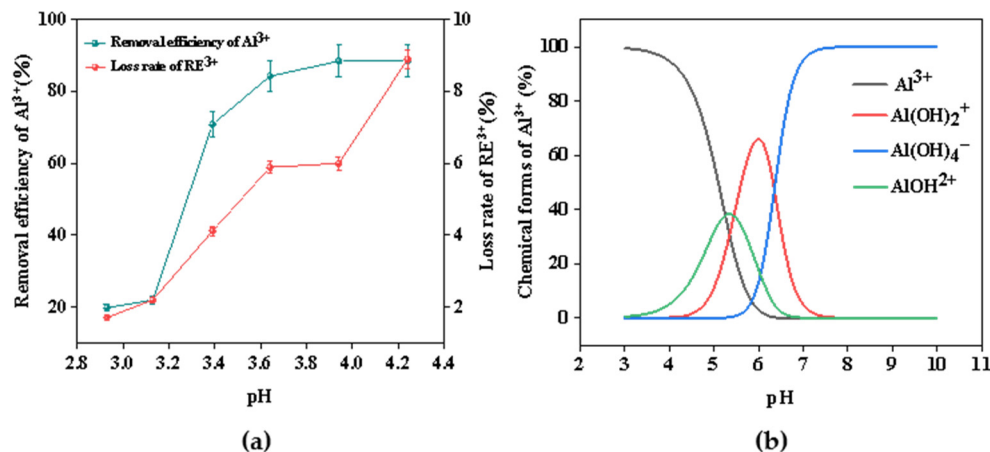


Figure 5. (a) Effect of final pH on the removal efficiency of Al^{3+} and loss rate of RE^{3+} ; (b) the main forms of $\text{Al}(\text{III})$ in solution at different pH values calculated via Visual MINTEQ.

3.1.4. Distribution of RE and Al

Hydrolysis transpires not only on the cathode surface, but also in the bulk solution [27]. Consequently, it is necessary to investigate the distribution of elements in both the plate and solution during electrochemical hydrolysis to optimize the experimental conditions. To ensure the precision of experimental outcomes and investigate the distribution of elements, a comparative analysis was conducted on the concentrations of each rare earth element and aluminum element pre-experiment and post-experiment. The result is shown in Figure 6a. Firstly, the total quantity of rare earth and aluminum impurities prior to the experiment was compared with the cumulative amount of these impurities in the solution, on the plate, and in post-experimental precipitation. The data from both measurements were found to be largely consistent, thereby validating the precision of the test results. On the other hand, for the distribution of rare earth and aluminum in different media, it could be found that after the electrochemical selective water dissolved aluminum, most of the rare earth remained in the solution, which was consistent with the previous experimental test results. Normally, the direct hydrolysis of rare earth near the electrode is the main factor causing the loss of rare earth [27]. In the electrochemical precipitation process, if the alkali production rate does not match the precipitation rate, the excess OH^- accumulates on the cathode plate, resulting in a local over-alkali phenomenon. As shown in Figure 6b, pH values at different distances in the cathodic solution were examined. The pH near the cathode plate was much higher than in the bulk solution, resulting in significant loss of rare earths. As the cathode plate was a smooth plane, the hydrolysate settled to the bottom of the solution under the action of mechanical agitation and mass transfer, forming a large hydrogen oxidation precipitate. Since the pH of the solution exceeded the pH at which aluminum began to precipitate, the hydrolysis of aluminum ions occurred mainly in the bulk solution. Therefore, in order to reduce the loss rate of rare earth and improve the removal rate of aluminum, on the one hand, mechanical agitation in the electrochemical precipitation of aluminum was increased to reduce local alkali. In addition, by adjusting the current density, the rate of alkali production was matched to the hydrolysis rate to reduce the accumulation of OH^- ions.

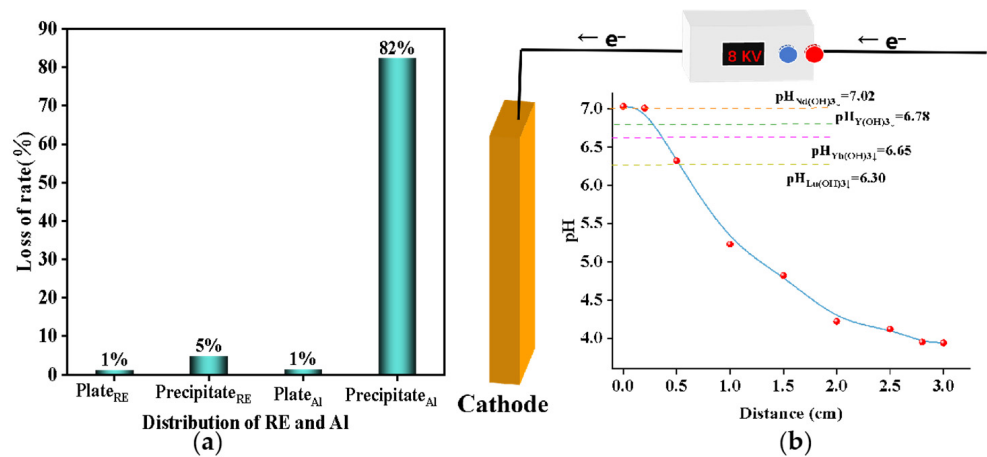


Figure 6. (a) Distribution of rare earth elements and aluminum elements in different media; (b) the pH values at different distances in the cathodic solution.

3.2. Mechanism

3.2.1. Precipitation Kinetics of Al³⁺

In the electrochemical precipitation process, the removal of aluminum followed the pseudo-zero order reaction model at low current density and the pseudo-first order kinetic model at high current density [27]. According to the electrochemical mechanism, the rate of OH⁻ ion generation was slow at low current density which was basically equal to the rate of ion precipitation. It was consistent with the zero-order reaction, where the reaction rate was independent of the concentration of the reactants. At high current densities, the hydroxyl formation rate was much higher than the ion precipitation reaction rate, resulting in the accumulation of a large amount of OH⁻, making the reaction equilibrium occur towards the forward reaction, and the reaction rate was related to the concentration of the reactant. In order to predict the precipitation kinetic model of aluminum ions, the relationship between aluminum concentration and time was investigated as shown in Figure 7. The concentration of aluminum ions decreased with the increase in time.

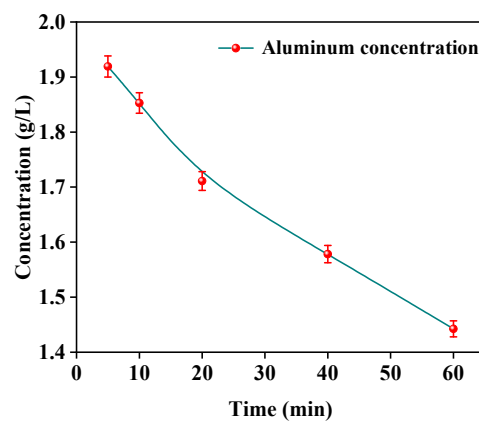


Figure 7. Time versus the Al³⁺ concentrations.

The relationship between aluminum ion concentration and time was fitted using the pseudo-zero order model of Equation (10) and the pseudo-first order model of Equation (11) to further describe the precipitation kinetics of aluminum removal.

$$C_0 - C = k_0t \tag{10}$$

$$\ln C_0 - \ln C = k_1t \tag{11}$$

where C_0 is the concentration of Al^{3+} ions before precipitation started, and C is the Al^{3+} concentration measured at time t . k_0 ($mg \cdot L^{-1} \cdot min^{-1}$) and k_1 (min^{-1}) are the rate constants of the pseudo zero-order model and the pseudo first-order model, respectively; t (min) is the reaction time for Al removal.

Comparing the R^2 values of the two models (Figure 8a,b), it was found that good correlation coefficients were obtained for the pseudo-first order kinetic model, which shows that the precipitation process of aluminum followed the pseudo first-order rate expression, meaning that the reaction rate was proportional to the first square of the reactant concentration, and the rate constant was 0.005 min^{-1} .

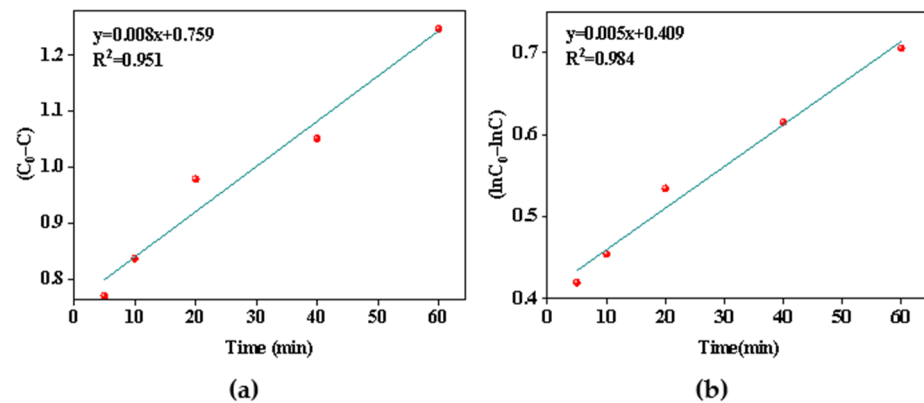


Figure 8. (a) Pseudo-zero order model of the Al removal; (b) pseudo-first-order model of the Al removal.

3.2.2. SEM Analysis

The Scanning Electron Microscope (SEM) of the precipitation after filtration by impurity removal is shown in Figure 9. Table 3 shows the EDS results of precipitation under optimal conditions. The results indicate that the SEM image of precipitation predominantly features flocculent amorphous precipitation. These precipitates were irregularly dispersed within fine particles and exhibit significant hardening and caked formation. It was speculated that the morphology was mainly caused by the combination of aluminum hydroxide and rare earth hydroxide deposits. This is in agreement with the results reported in the literature for the removal of aluminum from rare earth solutions by the use of other precipitating agents [33]. Table 3 further revealed that the primary constituents of the precipitation were aluminum hydroxide, with a minor presence of rare earth attached to the precipitation surface. Consequently, employing electrochemical selective hydrolysis proved effective in eliminating aluminum ions present in the rare earth solution. Concurrently, this method reduced the loss induced by the co-precipitation of rare earth and impurities.

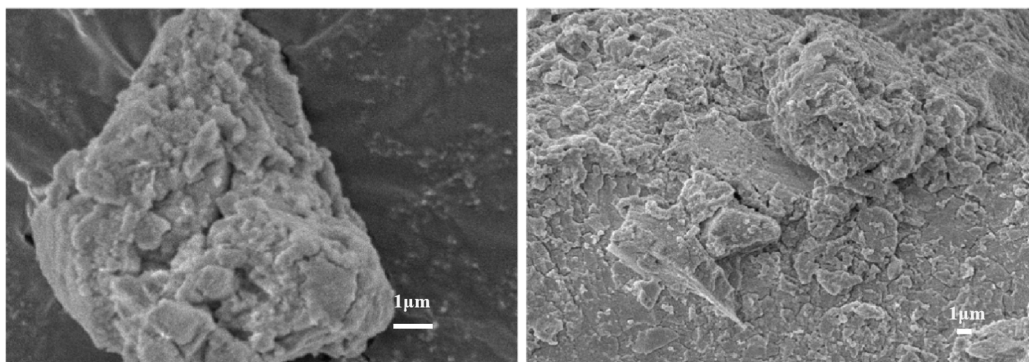


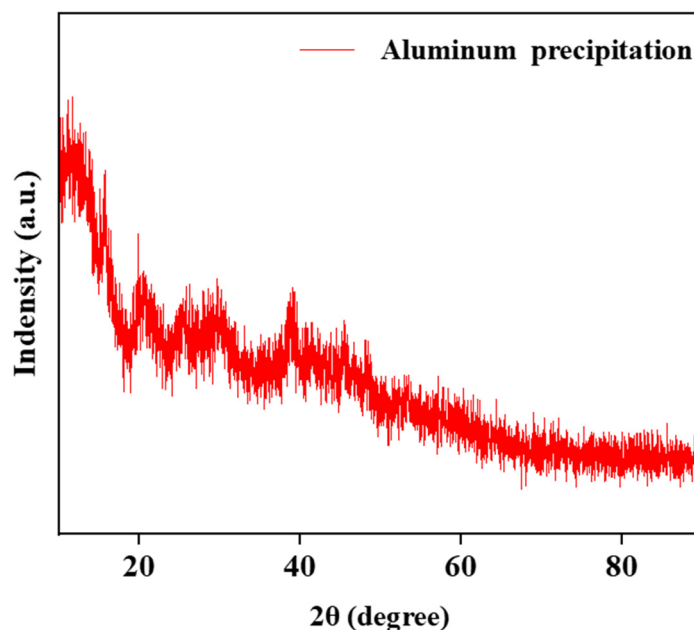
Figure 9. The SEM of aluminum precipitation.

Table 3. EDS analysis results of precipitation under optimal conditions.

Elements	Wt%
O	29.85
Al	23.24
Cl	15.86
La	3.94
Nd	3.48
Dy	0.90
Y	1.88
Others	20.85

3.2.3. XRD Analysis

The structure of the aluminum hydroxide precipitated from the solution is strongly influenced by the pH of the solution. Aluminum hydroxide with different crystalline forms were synthesized under different pHs. With the increase in pH from 3 to 12, the generated aluminum hydroxides were amorphous, boehmite [γ -AlOOH], and bayerite [α -Al(OH)₃], respectively [34,35]. The results in Figure 10 show that the structure of precipitation was demonstrated via XRD as an amorphous phase.

**Figure 10.** The XRD analysis of aluminum precipitation.

3.2.4. TEM Analysis

Further analysis of the separated precipitates was carried out by accurate characterization of their crystal structure using Transmission Electron Microscope (TEM). TEM images shown that the sediment was flocculent and amorphous, with no crystalline characteristics. The aluminum content in the EDS images was significantly higher than that of other substances. In the RECl₃ solution, the concentrations of La, Nd and Y were 22.76 g·L⁻¹, 24.13 g·L⁻¹ and 32.70 g·L⁻¹, respectively. However, compared with the above elements, the concentrations of other elements were much lower. This may be the reason why the rare earth elements with low concentration on the surface could not be detected by EDS. The feasibility of electrochemical selective precipitation for separation of aluminum impurities and the precipitation as amorphous with no degree of crystallinity and crystalline features were confirmed based on the TEM image of ground hydroxides shown in Figure 11 and the selected area EDS image shown in Figure 12.

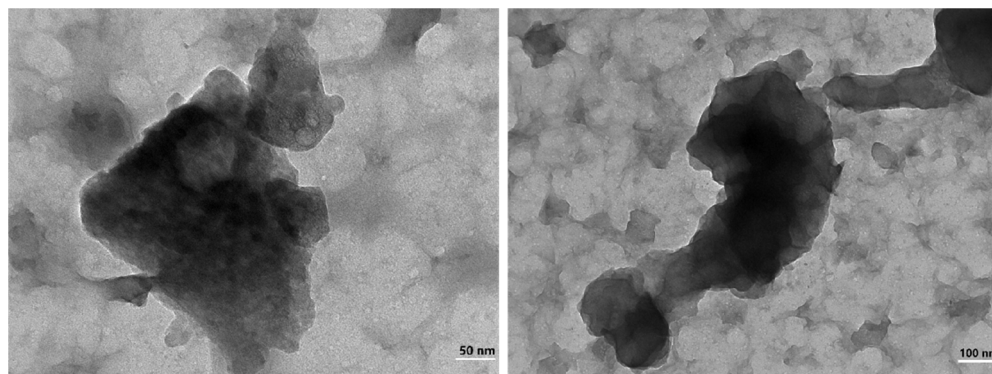


Figure 11. The TEM of aluminum precipitation.

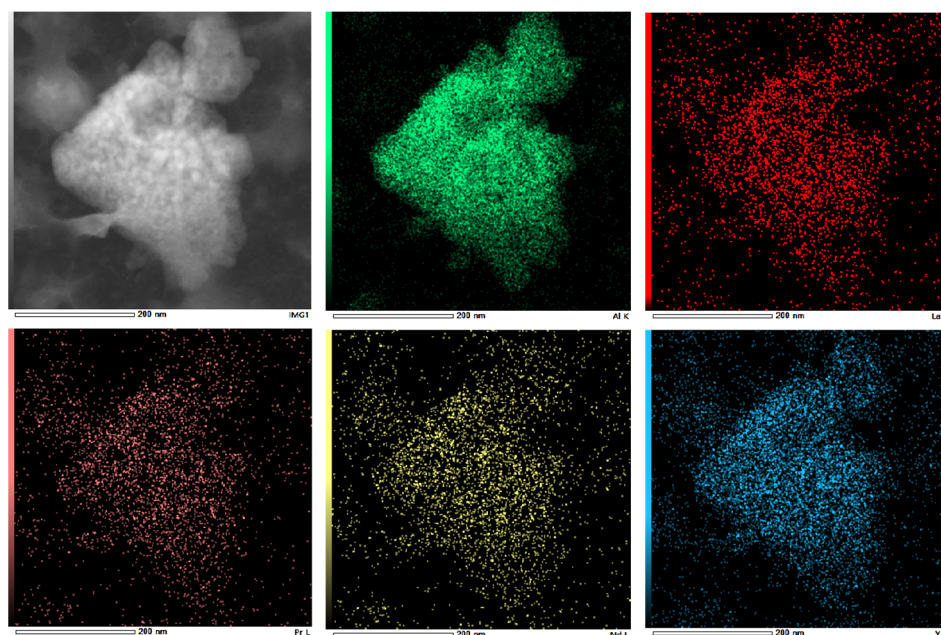


Figure 12. The EDS of aluminum precipitation.

3.3. Comparison and Energy Consumption

Under the same conditions, aluminum in rare earth chloride solution was removed by adding ammonia directly and the results compared with this method are shown in Table 4. From Table 4 and Figure 13, it can be observed that at an equivalent pH level, the efficiency of selective hydrolysis in removing aluminum surpassed that of traditional neutralization hydrolysis. Furthermore, a lower loss rate of rare earth was obtained. At present, the main methods for removing Al from rare earth leachate are selective precipitation and solvent extraction. NH_4HCO_3 was a conventional precipitate of Al removal. The electrochemical precipitate process was compared with NH_4HCO_3 precipitation methods. The results are shown in Table 5. A significant reduction in RE loss was achieved via electrochemical precipitate. Other selective precipitate methods mentioned in the existing literature were also compared as shown in Table 5. Solvent extraction was proved to be an efficient method for the separation of rare earth elements and Al(III) impurity. The comparison between solvent extraction and this work is shown in Table 6. Our work aimed at providing a new alternative strategy for efficient and green separation of Al(III) impurity from complex rare earth leachate.

Table 4. Comparison of aluminum removal efficiency via different methods.

Method	Removal Efficiency of Al ³⁺	Loss Rate of RE ³⁺
Electrochemical regulated hydrolysis	88.35%	5.99%
Adding ammonia	85.04%	11.15%

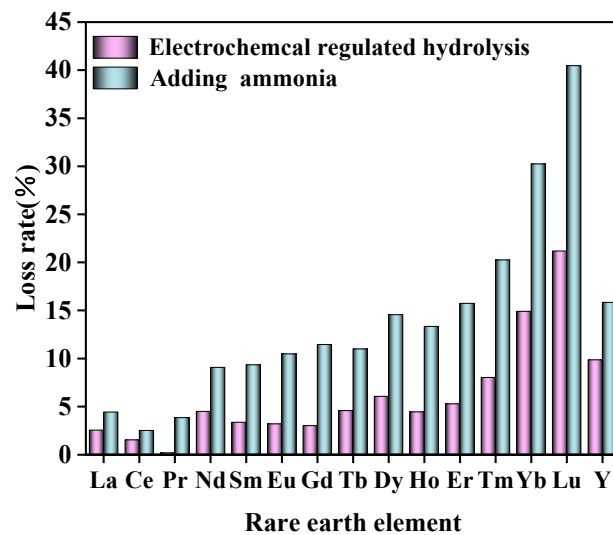


Figure 13. Comparison of the loss rate of rare earth via electrochemical regulated hydrolysis and adding ammonia.

Table 5. The comparison between selective precipitation method and this work.

Literature	Precipitant	Feed Materials	Summary
[27]	NH ₄ HCO ₃	The real ionic rare earth leachate obtaining by MgSO ₄ solution leaching (C _{Al} ³⁺ = 30.6 mg·L ⁻¹ ~161.1 mg·L ⁻¹ , C _{RE} ³⁺ = 215.7 mg·L ⁻¹)	The removal efficiency of Al (III) impurity was 86.3% while 7.0% of rare earth was lost
[22]	8-hydroxyquinoline	A leaching solution of rare-earth concentrate ore by hydrochloric acid was used as the experimental raw material (C _{Al} ³⁺ = 0.6 g·L ⁻¹ , C _{RE} ³⁺ = 75 g·L ⁻¹)	The Al ³⁺ removal reached 94.39%, and the loss ratio of RE ³⁺ was only 8.21%
[33]	Decyl glucoside (DG)	The low concentration rare earth lixivium, which was leached by magnesium sulfate leaching process (C _{Al} ³⁺ = 208.2 mg·L ⁻¹ , C _{RE} ³⁺ = 586.3 mg·L ⁻¹)	The aluminum removal rate of lixivium kept over 95% and the rare earth loss rate was around 7%
This work		The real ionic rare earth leachate obtaining by HCl solution leaching (C _{Al} ³⁺ = 5.42 g·L ⁻¹ , C _{RE} ³⁺ = 197.91 g·L ⁻¹)	The removal efficiency of Al (III) impurity was 88.35% while 5.99% of rare earth was lost under optimal conditions

Energy consumption is one of the most important parameters affecting the economics of electrochemical precipitation. The energy consumption E (kw/ton_(RECl₃)) for electrochemical precipitation of 1 ton of feed liquid can be calculated as follows:

$$EV = UIt \tag{12}$$

where U is the voltage in the electrolysis process and I is the current in the electrolysis process. t is the time required for the electrochemical precipitation process.

With higher current densities applied and consequently higher voltage, the amount of energy required was considerably greater (Figure 14). After comprehensive consideration of optimized conditions, the energy consumption of one ton of rare earth chloride solution in this study was 23.1 kw.

Table 6. The comparison between solvent extraction and this work.

Literature	Extractant	Feed Materials	Summary
[16]	4-octoxybenzoic acid	The simulated rare earth solution ($C_{RE^{3+}} = 0.3 \text{ mol}\cdot\text{L}^{-1}$, $C_{Al^{3+}} = 0.04 \text{ mol}\cdot\text{L}^{-1}$)	The separation factor of Al^{3+} and RE^{3+} reached 75.03 at 50 °C
[10]	3-((bis(2-ethylhexyloxy))phosphoryl)-3-phenylpropanoic acid	The simulated $RECl_3$ solution containing Sm^{3+} , Lu^{3+} , Y^{3+} and Al^{3+} ($C_{RE^{3+}} = 0.03 \text{ mol}\cdot\text{L}^{-1}$, $C_{Al^{3+}} = 0.01 \text{ mol}\cdot\text{L}^{-1}$)	The removal rate of Al^{3+} was up to 98% and the loss of RE was less than 5%
[36]	[N1888][C7H11O2]	The industrial $GdCl_3$ feed solution ($C_{Gd^{3+}} = 146 \text{ g}\cdot\text{L}^{-1}$, $C_{Al^{3+}} = 762 \text{ mg}\cdot\text{L}^{-1}$)	The removal rate of Al^{3+} was up to 98.69% and the recovery rate of Gd^{3+} achieved at 92.47%
[37]	$[(CH_2)_nCOOHpyr][NTf_2]$, $n = 3, 5, 7$ and [C4mim][NTf2]	The industrial solutions containing $GdCl_3$ (~2639 mg/L) with $Al(III)$ impurity (~434 mg/L) and $GdCl_3$ (~2976 mg/L) with $Al(III)$ impurity (~331 mg/L)	The removal efficiency of Al (III) impurity was 99.3% and at the same time, more than 30% of Gd^{3+} was co-extracted
This work		The real ionic rare earth leachate obtaining by HCl solution leaching ($C_{Al^{3+}} = 5.42 \text{ g}\cdot\text{L}^{-1}$, $C_{RE^{3+}} = 197.91 \text{ g}\cdot\text{L}^{-1}$)	The removal efficiency of Al (III) impurity was 88.35% while 5.99% of rare earth was lost under optimal conditions

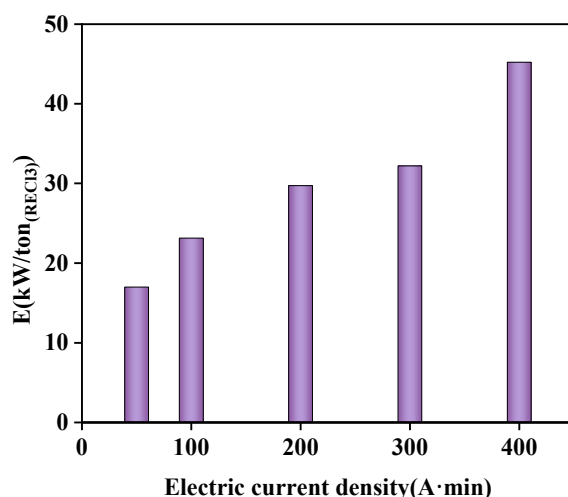


Figure 14. Effect of different current densities on energy consumption.

3.4. Green Evaluation of the Proposed Methodology

Over the past few decades, there has been a significant increase in interest regarding the impact of analytical chemistry on various facets such as environmental considerations, operational procedures, and the utilization of solvents, reagents, and energy resources [38]. Researchers and industry professionals are actively exploring alternative solvents and reagents that are less harmful to the environment, as well as ways to reduce energy consumption in chemical processes. In addition, governments and regulatory bodies are placing greater emphasis on the assessment and control of chemicals to reduce their adverse effects on the environment and human health [39]. The green analytical procedure index (GAPI) [40] and the analytical greenness metric for sample preparation (AGREEprep) [41] can be considered as the most widely used method greenness assessment criteria. The obtained evaluations are shown in Figure 15. As shown in Figure 15a, the sample preparation treatment using the AGREEprep procedure scored 0.73 points. However, sample preparation is only one part of the overall experimental process, and when analyzing the whole experiment, the AGREE procedure is the better green evaluation tool. As shown in Figure 15b, taking into account the 12 Green Analytical Chemistry Guidelines and the Importance Principle, the AGREE tool assigns a score of 0.71 to the proposed method. In contrast, with direct precipitation, such as the addition of ammonia to the solution for the removal of aluminum impurities, green evaluation was performed under the same

conditions. According to the calculations of AGREEprep and AGREE, the values are 0.55 and 0.64, respectively (see Figure 15c,d). The electrochemical regulated hydrolysis process had a higher degree of green evaluation and was more environmentally friendly and pollution-free.

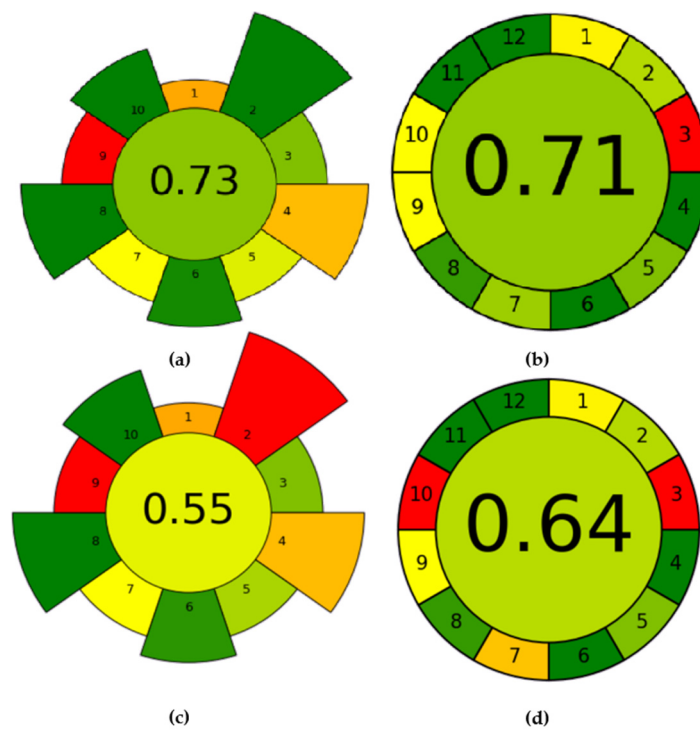


Figure 15. (a) Results of regulated hydrolysis AGREEprep analysis; (b) results of regulated hydrolysis AGREE assessment; (c) results of adding ammonia AGREEprep analysis; (d) results of adding ammonia AGREE assessment.

4. Conclusions

Electrochemical regulating hydrolysis under electric field was successfully used for selective precipitation separation of Al^{3+} from a rare earth chloride solution in this study. It displayed the advantages of high selectivity, regulatability, and less rare earth loss during the precipitation process; the main conclusions were as follows:

In the present study, it was determined that the optimal conditions were 25 °C reaction temperature, 100 A/m^2 current density, and 3.90 final pH level. The procedure yielded a commendable result, with an efficiency rate of 88.35% for aluminum removal and a rare earth loss rate of merely 5.99%. A kinetic analysis of aluminum precipitation revealed that the reaction adhered to pseudo-first order kinetics. Additionally, the precipitate obtained via separation and filtration was amorphous alumina hydroxide with a small amount of rare earth attached. The AGREEprep and AGREE assessment tools were used to make a green assessment of this method and the scores were 0.73 and 0.71, respectively. The energy consumption of one ton of rare earth chloride solution in this study was 23.1 $\text{kW}/\text{ton}_{(\text{RECl}_3)}$. Furthermore, the final scores for aluminum removal using the traditional neutralization hydrolysis process were 0.55 and 0.64, respectively. This study provided an effective, economical, and clean method for the removal of aluminum from a solution of rare earth elements.

Author Contributions: Y.Z.: Data curation, Investigation, Methodology, Validation, Writing original draft. J.L.: Writing original draft, Funding acquisition, Article revision, Supervision. D.X.: Investigation. M.L.: Investigation, Article revision. B.X.: Investigation, Methodology. X.Z.: Article revision. Y.X.: Article revision. H.Z.: Funding, Supervision, Review and editing. T.Q.: Project administration, Funding, Supervision. All authors have read and agreed to the published version of the manuscript.

Funding: This work was financially supported by the Natural Science Youth Foundation of Jiangxi Province (No. 20212BAB213031), the General Project of the Key Research and development Program of Ganzhou (Nos. 202101124952 and 202101124954), the Double Thousand Plan of Jiangxi Province (jxsq2020105012), the National Natural Science Foundation of China (No. 22268048), National Key Research and Development Program of China (No. 2022YFB3504300), a grant from the Research Projects of Jiangxi Institute of Rare Earths, Chinese Academy of Sciences (E055ZA01).

Data Availability Statement: Data are contained within the article.

Conflicts of Interest: The authors declare that they have no known competing financial interests or personal relationships that could have appeared to influence the work reported in this paper.

References

1. Traore, M.; Gong, A.; Wang, Y.; Qiu, L.; Bai, Y.; Zhao, W.; Liu, Y.; Chen, Y.; Liu, Y.; Wu, H. Research progress of rare earth separation methods and technologies. *J. Rare Earths* **2023**, *41*, 182–189. [[CrossRef](#)]
2. Opere, E.O.; Struhs, E.; Mirkouei, A. A comparative state-of-technology review and future directions for rare earth element separation. *Renew. Sustain. Energy Rev.* **2021**, *143*, 110917. [[CrossRef](#)]
3. Chen, Z.; Li, Z.; Chen, J.; Kallem, P.; Banat, F.; Qiu, H. Recent advances in selective separation technologies of rare earth elements: A review. *J. Environ. Chem. Eng.* **2022**, *10*, 107104. [[CrossRef](#)]
4. Rahman, M.H.; Rahaman, M.Z.; Chowdhury, E.H.; Motalab, M.; Hossain, A.A.; Roknuzzaman, M. Understanding the role of rare-earth metal doping on the electronic structure and optical characteristics of ZnO. *Mol. Syst. Des. Eng.* **2022**, *7*, 1516–1528. [[CrossRef](#)]
5. Boskovic, C. Rare earth polyoxometalates. *Acc. Chem. Res.* **2017**, *50*, 2205–2214. [[CrossRef](#)] [[PubMed](#)]
6. Lv, R.; Raab, M.; Wang, Y.; Tian, J.; Lin, J.; Prasad, P.N. Nanochemistry advancing photon conversion in rare-earth nanostructures for theranostics. *Coord. Chem. Rev.* **2022**, *460*, 214486. [[CrossRef](#)]
7. He, Q.; Qiu, J.; Chen, J.; Zan, M.; Xiao, Y. Progress in green and efficient enrichment of rare earth from leaching liquor of ion adsorption type rare earth ores. *J. Rare Earths* **2022**, *40*, 353–364. [[CrossRef](#)]
8. Xie, F.; Zhang, T.A.; Dreisinger, D.; Doyle, F. A critical review on solvent extraction of rare earths from aqueous solutions. *Miner. Eng.* **2014**, *56*, 10–28. [[CrossRef](#)]
9. Judge, W.D.; Azimi, G. Recent progress in impurity removal during rare earth element processing: A review. *Hydrometallurgy* **2020**, *196*, 105435. [[CrossRef](#)]
10. Wu, G.; Liao, W. Removal of aluminum from chloride leach solutions of rare earths using 3-((bis (2-ethylhexyloxy)) phosphoryl)-3-phenylpropanoic acid (PPPA). *Hydrometallurgy* **2022**, *208*, 105825. [[CrossRef](#)]
11. Qiu, T.; Wu, H.; Fang, X.; Li, X. The current situation and trends of the technology for impurity removal of weathering crust ion-absorbed type rare earth ores. *Xitu Chin. Rare Earths* **2012**, *33*, 81–85.
12. Zhang, W.; Xie, X.; Tong, X.; Du, Y.; Song, Q.; Feng, D. Study on the effect and mechanism of impurity aluminum on the solvent extraction of rare earth elements (Nd, Pr, La) by P204-P350 in chloride solution. *Minerals* **2021**, *11*, 61. [[CrossRef](#)]
13. Wu, W.; Zhang, F.; Bian, X.; Xue, S.; Yin, S.; Zheng, Q. Effect of loaded organic phase containing mixtures of silicon and aluminum, single iron on extraction of lanthanum in saponification P507-HCl system. *J. Rare Earths* **2013**, *31*, 722–726. [[CrossRef](#)]
14. Yang, X.; Qiu, T. Influence of aluminum ions distribution on the removal of aluminum from rare earth solutions using saponified naphthenic acid. *Sep. Purif. Technol.* **2017**, *186*, 290–296. [[CrossRef](#)]
15. Zeng, Z.; Gao, Y.; Liu, C.; Sun, X. A novel functionalized ionic liquid [DOC4mim][DEHG] for impurity removal of aluminum in rare earth leaching solution. *Sep. Purif. Technol.* **2022**, *296*, 121388. [[CrossRef](#)]
16. Yu, G.; Zeng, Z.; Gao, Y.; Ni, S.; Zhang, H.; Sun, X. Separation of aluminum from rare earth by solvent extraction with 4-octyloxybenzoic acid. *J. Rare Earths* **2023**, *41*, 290–299. [[CrossRef](#)]
17. Chi, R.; Zhou, Z.; Xu, Z.; Hu, Y.; Zhu, G.; Xu, S. Solution-chemistry analysis of ammonium bicarbonate consumption in rare-earth-element precipitation. *Metall. Mater. Trans. B* **2003**, *34*, 611–617. [[CrossRef](#)]
18. Wang, J.; Huang, X.; Wang, L.; Wang, Q.; Yan, Y.; Zhao, N.; Cui, D.; Feng, Z. Kinetics study on the leaching of rare earth and aluminum from FCC catalyst waste slag using hydrochloric acid. *Hydrometallurgy* **2017**, *171*, 312–319. [[CrossRef](#)]
19. Silva, R.G.; Morais, C.A.; Teixeira, L.V.; de Oliveira, É.D. Selective removal of impurities from rare earth sulphuric liquor using different reagents. *Miner. Eng.* **2018**, *127*, 238–246. [[CrossRef](#)]
20. Silva, R.G.; Morais, C.A.; Oliveira, É.D. Selective precipitation of rare earth from non-purified and purified sulfate liquors using sodium sulfate and disodium hydrogen phosphate. *Miner. Eng.* **2019**, *134*, 402–416. [[CrossRef](#)]
21. Tunsu, C.; Petranikova, M.; Ekberg, C.; Retegan, T. A hydrometallurgical process for the recovery of rare earth elements from fluorescent lamp waste fractions. *Sep. Purif. Technol.* **2016**, *161*, 172–186. [[CrossRef](#)]
22. Wang, Y.; Li, J.; Gao, Y.; Yang, Y.; Gao, Y.; Xu, Z. Removal of aluminum from rare-earth leaching solutions via a complexation-precipitation process. *Hydrometallurgy* **2020**, *191*, 105220. [[CrossRef](#)]
23. Falagán, C.; Yusta, I.; Sánchez-España, J.; Johnson, D.B. Biologically-induced precipitation of aluminum in synthetic acid mine water. *Miner. Eng.* **2017**, *106*, 79–85. [[CrossRef](#)]

24. Ntuk, U.; Tait, S.; White, E.T.; Steel, K.M. The precipitation and solubility of aluminum hydroxyfluoride hydrate between 30 and 70 °C. *Hydrometallurgy* **2015**, *155*, 79–87. [[CrossRef](#)]
25. Allahkarami, E.; Rezai, B. A literature review of cerium recovery from different aqueous solutions. *J. Environ. Chem. Eng.* **2021**, *9*, 104956. [[CrossRef](#)]
26. Zeppenfeld, K. Electrochemical removal of calcium and magnesium ions from aqueous solutions. *Desalination* **2011**, *277*, 99–105. [[CrossRef](#)]
27. Xie, D.; Li, J.; Zhang, H.; Zhu, Y.; Zhang, X.; Liu, K.; Xie, Y.; Qi, T.; Huang, Z. A novel electrochemical method for the removal of aluminum from ionic rare earth leachate. *Sep. Purif. Technol.* **2024**, *345*, 127296. [[CrossRef](#)]
28. Miller, S.E.; Heath, G.R.; Gonzalez, R.D. Effects of temperature on the sorption of lanthanides by montmorillonite. *Clays Clay Miner.* **1982**, *30*, 111–122. [[CrossRef](#)]
29. Miller, S.E.; Heath, G.R.; Gonzalez, R.D. Effect of pressure on the sorption of Yb by montmorillonite. *Clays Clay Miner.* **1983**, *31*, 17–21. [[CrossRef](#)]
30. Lei, Y.; Zhan, Z.; Saakes, M.; Weijden, R.D.; Buisman, C.J. Electrochemical recovery of phosphorus from acidic cheese wastewater: Feasibility, quality of products, and comparison with chemical precipitation. *ACS EST Water* **2021**, *1*, 1002–1013. [[CrossRef](#)]
31. Jin, H.; Yu, Y.; Zhang, L.; Yan, R.; Chen, X. Polarity reversal electrochemical process for water softening. *Sep. Purif. Technol.* **2019**, *210*, 943–949. [[CrossRef](#)]
32. Wang, D.; Hu, Y. *Solution Chemistry of Flotation*; Hunan Science and Technology Press: Changsha, China, 1988; Volume 6, pp. 132–179.
33. Zhou, H.; Xie, F.; He, K.; Zhang, Y.; Luo, X. Significantly enhance the removal of aluminum from yttrium rich rare earth lixivium by using decyl glucoside as precipitant. *Miner. Eng.* **2023**, *195*, 108044. [[CrossRef](#)]
34. Du, X.; Wang, Y.; Su, X.; Li, J. Influences of pH value on the microstructure and phase transformation of aluminum hydroxide. *Powder Technol.* **2009**, *192*, 40–46. [[CrossRef](#)]
35. Yang, Y.; Jiang, S.; Li, J.; Long, X. Analysis of the effect of pH on the crystal form of aluminum hydroxide. *Inorg. Salt Ind.* **2017**, *49*, 39–41.
36. Zhang, N.; Li, F.; Hu, K.; Wang, Z.; Xue, H.; Fan, B.; Zhang, X.; Dong, H. Selective separation Al³⁺/Gd³⁺ by designed carboxylic acid-ionic liquid with low acid and alkali consumption. *Sep. Purif. Technol.* **2023**, *318*, 123853. [[CrossRef](#)]
37. Hu, K.; Xing, L.; Nie, Y.; Li, X.; Dong, H.; Gao, H. Removal of aluminum to obtain high purity gadolinium with pyridinium-based ionic liquids. *Hydrometallurgy* **2022**, *213*, 105930. [[CrossRef](#)]
38. Gallart-Mateu, D.; Gallardo, A.; Garrigues, S.; Guardia, M. A green methodology for the determination of cocaine in camouflaged samples. *Anal. Methods* **2023**, *15*, 1969–1978. [[CrossRef](#)] [[PubMed](#)]
39. Anastas, P.; Eghbali, N. Green chemistry: Principles and practice. *Chem. Soc. Rev.* **2010**, *39*, 301–312. [[CrossRef](#)] [[PubMed](#)]
40. Płotka-Wasyłka, J. A new tool for the evaluation of the analytical procedure: Green Analytical Procedure Index. *Talanta* **2018**, *181*, 204–209. [[CrossRef](#)]
41. Wojnowski, W.; Tobiszewski, M.; Pena-Pereira, F.; Psillakis, E. AGREEprep—Analytical greenness metric for sample preparation. *TrAC Trends Anal. Chem.* **2022**, *149*, 116553. [[CrossRef](#)]

Disclaimer/Publisher’s Note: The statements, opinions and data contained in all publications are solely those of the individual author(s) and contributor(s) and not of MDPI and/or the editor(s). MDPI and/or the editor(s) disclaim responsibility for any injury to people or property resulting from any ideas, methods, instructions or products referred to in the content.